

Microscopic Optically Powered Bubble Rockets

CNF Project Number: 900-00

Principal Investigator(s): Paul L. McEuen

User(s): Samantha L. Norris, Michael F. Reynolds

Affiliation(s): Physics, Cornell University

Primary Source(s) of Research Funding: Cornell Center for Materials Research (DMR-1719875)

Contact: plm23@cornell.edu, sn588@cornell.edu, mfr74@cornell.edu

Primary CNF Tools Used: ABM Contact Aligner, Oxford Cobra/81/82/100 Etchers,
Oxford ALD/PECVD, Heidelberg Mask Writer - DWL2000

Abstract:

Bubble propulsion as a swimming mechanism for artificial microswimmers has been of significant interest recently, especially for biomedical applications. We demonstrate hundred-micron-scale bubble-propelled microswimmers that produce bubbles via voltage-induced water electrolysis, allowing operation in any aqueous solution, including physiological saline. These bubble rockets are powered by onboard photodiodes, allowing individual addressability limited only by the power and divergence of the light beam. We also demonstrate the ability to design microswimmers with different trajectories based on device geometry, and show integration with thin-film magnets for *in situ* steering. Finally, we present a novel method for locomotion on a solid-liquid interface.

Summary of Research:

We present hundred-micron-scale bubble rockets that consist of onboard photodiodes used to convert incident light into a voltage and current for water electrolysis. A diagram of a microswimmer is shown in Figure 1a. Each device consists of multiple silicon P-N junctions wired in series with two platinum electrodes roughly shaped like a tapered hollow cylinder with a rectangular cross section. Each photodiode has an open-circuit voltage of roughly 0.65V with a responsivity of ~ 0.3 A/W under Hg lamp illumination and operates in a light intensity of 1 kW/m^2 , roughly that of a sunny day. The entire device is encapsulated in silicon dioxide except for the interior of the hollow electrodes.

Under standard microscope illumination, the onboard photodiodes apply a voltage between the two electrodes sufficiently high to split water, producing hydrogen and oxygen gas at the cathode and anode respectively. The capillary force on these bubbles in the tapered cylinder forces them to be ejected from the tube, propelling the microswimmer forward.

A time lapse of a device swimming in 10 mM PBS is shown in Figure 1b, with a displacement vs. time curve

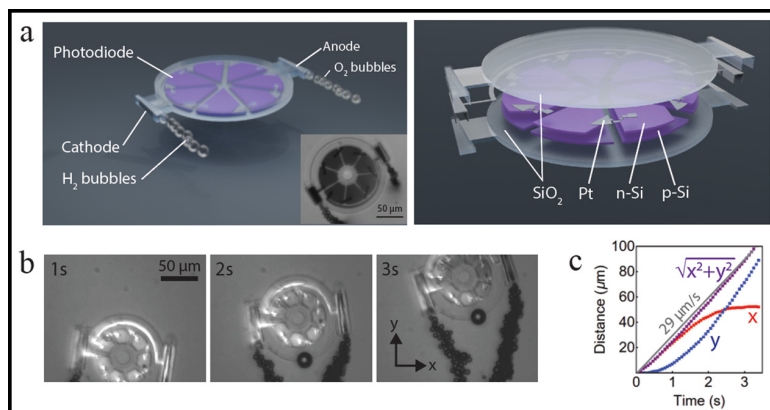


Figure 1: Diagrams and optical micrographs of optically powered microswimmer and time lapse of swimming behavior. a) Diagrams of optically powered microswimmer showing encapsulated photodiodes, hollow platinum electrodes, and bubble production. Inset: microswimmer operating on glass-water interface in 10 mM PBS solution under Hg lamp illumination. b) Time lapse of a device swimming under mercury lamp illumination at an air-water interface in 10 mM PBS solution. c) Displacement vs. time for the swimming device shown in b.

in Figure 1c. This bubble rocket is swimming at roughly $30 \mu\text{m/s}$ at an air-water interface. Due to the stoichiometric ratio of hydrogen to oxygen produced during water splitting, the instantaneous velocity of the hydrogen-producing cathode is twice that of the oxygen-producing anode, resulting in a circular trajectory.

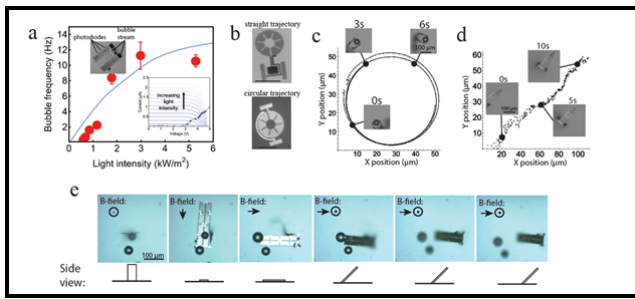


Figure 2: Description of microswimmer behavior. a) Measured bubble frequency as a function of incident light intensity for stationary microswimmer device (red) with expected bubble frequency from operating points in inset (blue). b) Micrographs of devices with circular and straight swimming trajectory showing wiring and electrode geometry. c) Time lapse and corresponding circular trajectory of a microswimmer with separate anodic and cathodic rockets on a solid-liquid interface. d) Time lapse and corresponding straight trajectory of a microswimmer with each rocket containing both anode and cathode on a liquid-liquid interface. e) Microswimmer on a solid-liquid interface with thin film magnets rotating in three dimensions and locomoting with an attack angle of 45 degrees to reduce friction.

The relationship between bubble ejection frequency and incident light intensity can be understood by considering separately the current-voltage characteristics of the photodiodes and on-chip rocket-shaped electrodes. The bubble ejection frequency for a microswimmer is shown in Figure 2a; the frequency increases with input light intensity until the photodiodes become voltage limited. The I-V curves of the photodiodes and on-chip electrodes are shown in the inset.

In addition, we demonstrate the ability to control microswimmer trajectory both by controlling electrode geometry and by integrating onboard thin film magnets for steering in a uniform magnetic field. The current required for bubble nucleation on an electrode depends on the confinement of the produced gas. Although both anode and cathode of the microswimmer must be exposed to fluid for current to flow, the placement and geometry of the electrodes can be designed to allow different swimming trajectories, as shown in Figure 2b. Circular and linear trajectories are shown for microswimmers in Figure 2c-d. By fabricating Co magnets onboard the microswimmers and performing experiments in a three-axis solenoid, the microswimmers can also be rotated and steered in three dimensions as shown in Figure 2e.

We have also shown the ability to engineer the microswimmer/substrate interface for more effective

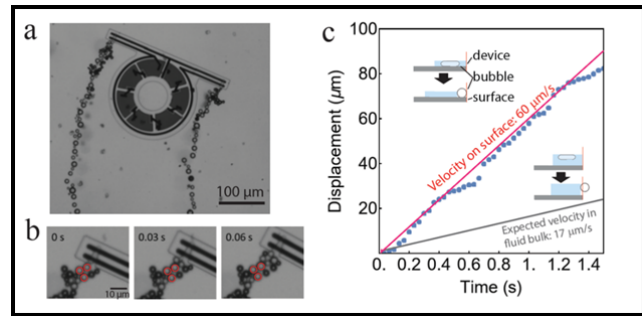


Figure 3: Utilizing bubble surface adhesion for increased surface swimming velocity. a) Micrograph of microswimmer locomoting on glass-water interface by pushing off ejected bubbles attached to the surface. b) Time lapse of microswimmer shown in (a) moving by approximately one bubble diameter with each bubble expulsion. c) Displacement as a function of time for device shown in (a) compared to maximum expected velocity using traditional bubble-propelled motion. Insets: diagrams showing mechanism of bubble propulsion for devices without (top) and with (bottom) a bottom on the rockets.

locomotion on a flat surface, as shown in Figure 3. By removing the bottom of the tube-shaped electrode, bubbles are able to attach to the surface and remain stationary while the capillary force of bubble growth propels the microswimmer forward. As such, the swimmer moves forward roughly one bubble diameter with each bubble expulsion, leaving the bubbles behind as shown in Figure 3a. A time lapse of the rocket movement is shown in Figure 3b. Each rocket contains both anode and cathode, such that the overall device moves forward in a straight line, with its trajectory shown in Figure 3c.

In conclusion, we have demonstrated a truly microscale bubble-propelled swimmer that can swim in physiological solutions with a long lifetime, paving the way for intelligent bubble-propelled microrobots to be used in applications from drug delivery, to manipulation, to *in vivo* monitoring. These bubble rockets can be fabricated to swim with a circular or linear trajectory and can also be integrated with thin-film magnets for steering in a uniform magnetic field. Finally, we have shown a novel method for bubble-propelled locomotion on a solid-liquid interface.